Mechanism of Lithium Dialkylamide-Mediated Ketone and Imine Deprotonations: An MNDO Study of Monomer and Open Dimer Pathways

Floyd E. Romesberg and David B. Collum*

Contribution from the Department of Chemistry, Baker Laboratory, Cornell University, Ithaca, New York 14853-1301

Received July 15, 1994[⊗]

Abstract: Lithium amide-mediated metalations of ketones and the corresponding *N*-alkylimines were studied through semiempirical (MNDO) calculations. We explored the influence of lithium amide, solvent, and substrate substituents on the absolute and relative stabilities of the monomer and open dimer transition structures. In general, relief of the high steric demands inherent to the disolvated cyclic dimer reactant structures upon proceeding to the transition structures is the dominant determinant of the activation enthalpies. The results shed light on a number of issues central to lithium amide-mediated metalations including the *syn* effect observed in imine metalations, *E*/*Z* ketone enolization selectivities, the dramatically reduced kinetic acidities of imines relative to ketones, and the role of the chelate effect in ligand-assisted imine metalations. Acyclic transition structures involving monomer, open dimer, and triple ion amide fragments implicate substantially different properties; however, their relatively high energy precluded detailed discussion.

Introduction

During the last three decades, lithium dialkylamide bases have emerged as the reagents of choice for the formation of lithium enolates and related stabilized carbanions.[1] An enormous number of empirical observations have formed the basis of frequent mechanistic debates. About eight years ago we initiated investigations of the structures and reactivities of lithium dialkylamides hoping to uncover the lithium dialkylamide structure−reactivity relationships underlying their role as strong Bronsted bases.[2−7] More recently we began to employ semiempirical (MNDO) computational methods to address a number of issues that could not be adequately addressed by spectroscopic and kinetic methods.[8,9] We have operated on the belief that success would depend critically on the capacity of MNDO to calculate geometries and stabilities of *chemically realistic* reactant and transition structures bearing the full complement of aggregate subunits, solvents, and alkyl substituents.[10]

Chart 1

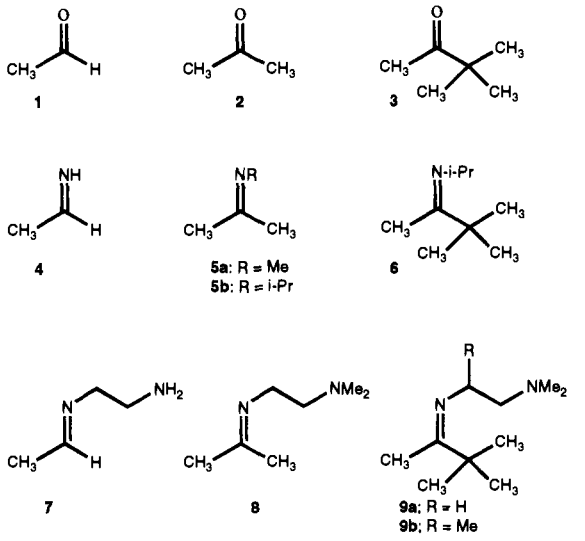

In this manuscript we describe MNDO computational studies of the lithiation of ketones (**1**−**3**), simple *N*-alkylimines (**4**−**6**), and *N*-alkylimines bearing potentially chelating NR_2 moieties (**7**−**9**) (Chart 1). The studies focussed upon a number of issues including: (1) the relative importance of aggregated and monomeric reactive intermediates; (2) the origins of *E*/*Z* ketone enolization selectivities; (3) the high kinetic acidity of ketones relative to the structurally related imines; (4) the "*syn* effect" in imine metalations, and (5) the role of chelation and the complex-induced proximity effect (CIPE)[11] on imine metalations. Extensive investigations of cyclic monomer- and open dimer-based pathways (corresponding to artists' renditions of

[⊗] Abstract published in *Advance ACS Abstracts,* November 15, 1994.

(1) d'Angelo, J. *Tetrahedron* **1976**, *32*, 2979. Heathcock, C. H. in *Comprehensive Carbanion Chemistry*; Buncel, E., Durst, T., Ed.; Elsevior: New York, 1980; Vol. B, Chapter 4. Cox, P. J.; Simpkins, N. S. *Tetrahedron: Asymmetry* **1991**, *2*, 1. *Asymmetric Synthesis*; Morrison, J. D., Ed.; Academic Press: New York, 1983; Vols. 2 and 3. Evans, D. A. in *Asymmetric Synthesis*; Morrison, J. D., Ed.; Academic Press: New York, 1983; Vol. 3, Ch. 1. Snieckus, V. *Chem. Rev.* **1990**, *90*, 879.

(2) Collum, D. B. *Acc. Chem. Res.* **1992**, *25*, 227.

(3) (a) Galiano-Roth, A. S.; Collum, D. B. *J. Am. Chem. Soc.* **1989**, *111*, 6772. (b) Bernstein, M. P.; Romesberg, F. E.; Fuller, D. J.; Harrison, A. T.; Collum, D. B.; Liu, Q.-Y.; Williard, P. G. *J. Am. Chem. Soc.* **1992**, *114*, 5100. (c) Bernstein, M. P.; Collum, D. B. *J. Am. Chem. Soc.* **1993**, *115*, 789. (d) Bernstein, M. P.; Collum, D. B. *J. Am. Chem. Soc.* **1993**, *115*, 8008.

(4) Hall, P.; Gilchrist, J. H.; Collum, D. B. *J. Am. Chem. Soc.* **1991**, *113*, 9571. Hall, P.; Gilchrist, J. H.; Harrison, A. T.; Fuller, D. J.; Collum, D. B. *J. Am. Chem. Soc.* **1991**, *113*, 9575. Galiano-Roth, A. S.; Kim, Y. J.; Gilchrist, J. H.; Harison, A. T.; Fuller, D. J.; Collum, D. B. *J. Am. Chem. Soc.* **1991**, *113*, 5053. Sakuma, K.; Gilchrist, J. H.; Romesberg, F. E.; Cajthaml, C. E. *Tetrahedron Lett.* **1993**, *34*, 5213. Depue, J. S.; Collum, D. B. *J. Am. Chem. Soc.* **1988**, *110*, 5518.

(5) Gilchrist, J. H.; Collum, D. B. *J. Am. Chem. Soc.* **1992**, *114*, 794.

(6) Romesberg, F. E.; Gilchrist, J. H.; Harrison, A. T.; Fuller, D. J.; Collum, D. B. *J. Am. Chem. Soc.* **1991**, *113*, 5751.

(7) Gregory, K.; Schleyer, P. v. R.; Snaith, R. *Adv. Inorganic Chem.* **1991**, *37*, 47. Mulvey, R. E. *Chem. Soc. Rev.* **1991**, *20*, 167.

(8) Romesberg, F. E.; Collum, D. B. *J. Am. Chem. Soc.* **1992**, *114*, 2112.

(9) Romesberg, F. E.; Collum, D. B. *J. Am. Chem. Soc.* **1994**, *116*, 9187.

(10) Dewar, M. J. S.; Jie, C. *Acc. Chem. Res.* **1992**, *25*, 537.

(11) Beak, P.; Meyers, A. I. *Acc. Chem. Res.* **1986**, *19*, 356.

0002-7863/95/1517-2166$09.00/0

Chart 2

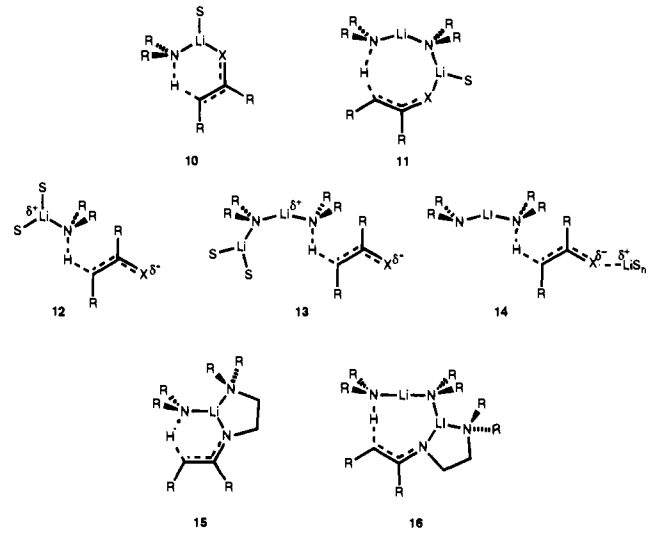

transition structures **10** and **11**; Chart 2) afford insight into mechanisms implicated in previous spectroscopic[6] and kinetic studies.[3] Investigations of acyclic transition structures (**12**, **13**) including metalations via triple ions (**14**) shed some light on several key experimental observations not adequately accounted for by cyclic transition structures.

Literature Background

Relative Reactivities of Imines and Ketones. Ketone enolates constitute one of the most important classes of reactive intermediate in synthetic organic chemistry.[12] The importance of lithioimines as ketone enolate equivalents is two-fold:[13] (1) The imine moiety contrasts with the analogous ketones by affording an *N*-alkyl substituent that allows one to modify reactivity and to impart desirable properties such as chirality; (2) proton abstractions from imines by lithium dialkylamides are extraordinarily slow, yet proceed smoothly without competing reversible proton transfers.[3] For example, the metalation of cyclohexanone by LDA is $\geq 10^3$ times faster than the corresponding reaction with cyclohexanone *N*-isopropylimine.[14] The origin of this large difference in reactivity has not been clearly articulated.

Aggregate vs Monomer Reactivity. The knowledge that organolithium derivatives form aggregates has been accompanied by a persistent debate about the relative reactivities of different aggregation states (whether observable or accessible only transiently).[15-17] It is an exceptional case when a combination of spectroscopic and kinetic data offers a clear demonstration of the degree of aggregation (and solvation) at the rate-limiting transition state.[18] In the case of lithium dialkylamides, early rate studies revealed fractional reaction orders consistent with deaggregation or other fragmentation events, yet were clouded by a persistent lack of details of solution structures.[19] Although odd stereo- and regioselectivities suggest that homonuclear and heteronuclear (mixed) aggregates may be important,[4,15] there exists no direct experimental distinction of monomer vs dimer reactivity in ketone enolate formation. However, LDA-mediated metalations of *N,N*-dimethylhydrazones (**17**) display well-defined half-order dependencies on LDA concentration.[3] Taken in conjunction with the recent assignment of LDA as a dimer in standard donor solvents,[3,5] the kinetics demonstrate the viability of monomer pathways. Initial mechanistic speculations included η^2-π-complexed intermediate **18** rather than η^1-σ complex **19**.[3a,b] The

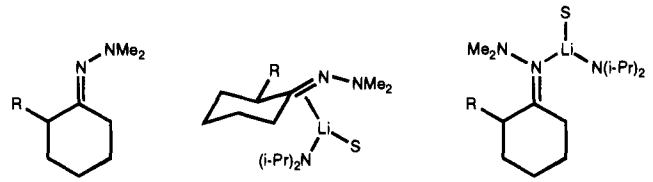

intermediacy of **18** was later questioned upon demonstration that the rate equation for metalations of the isostructural *N*-isopropylimines are of the same mathematical form.[3d] While the stoichiometry of the transition structure derived from intermediates such as **18** or **19** is established by the spectroscopic and rate studies, the implicit structural details have been based solely upon chemical intuition. One might ask why the metalations of the *N,N*-dimethylhydrazones and simple *N*-isopropylimines require deaggregation rather than proceeding directly from the LDA dimer. The importance of this question is underscored by computational,[8,9] spectroscopic,[6] and crystallographic[20] evidence that reaction via open dimers (e.g. **11**) analogous to those first proposed by Schlosser and co-workers[21] might be viable.[22] Thus, we hoped that semiempirical calculations would help us understand the relative efficacies of the monomer- and dimer-based metalation pathways.

The Chelate Effect. The advantages offered by chelation have been the topic of extensive discussion throughout orga-

(12) Williard, P. G. in *Comprehensive Organic Synthesis*; Pergamon: New York, 1991; Vol. 1, p 1. Jackman, L. M.; Bortiatynski, J. In *Advances in Carbanion Chemistry*; JAI: New York, 1992; Vol. 1, pp 45–87. Jackman, L. M.; Lange, B. C. *Tetrahedron* **1977**, *33*, 2737.

(13) Bergbreiter, D. E.; Momongan, M. In *Comprehensive Organic Synthesis*; Trost, B. M., Fleming, I., Ed.; Pergamon: New York, 1989; Vol. 1, p 503. Martin, S. F. *Ibid. Vol.* 1, p 475. Hickmott, P. W. *Tetrahedron* **1982**, *38*, 1975. Enders, D. In *Current Trends in Organic Synthesis*; Nozaki, H., Ed.; Pergamon: New York, 1983. Whitesell, J. K.; Whitesell, M. A. *Synthesis* **1983**, 517. Boche, G. *Angew. Chem., Int. Ed. Engl.* **1989**, *28*, 277.

(14) Gilchrist, J. H.; Remenar, J.; Collum, D. B. Unpublished.

(15) Seebach, D. *Angew. Chem., Int. Ed. Engl.* **1988**, *27*, 1624. Seebach, D. In *Proceedings of the Robert A. Welch Foundation Conferences on Chemistry and Biochemistry*; Wiley: New York, 1984. See also Caubere, P. In *Reviews of Heteroatom Chemistry*; MYU: Tokyo, 1991; Vol. 4, pp 78–139.

(16) *Ions and Ion Pairs in Organic Reactions*; Szwarc, M., Ed.; Wiley: New York, 1972; Vols. 1 and 2. Fraenkel, G.; Hsu, H.; Su, B. P. In *Lithium: Current Applications in Science, Medicine, and Technology*; Bach, R. O., Ed.; Wiley: New York, 1985; Chapter 19. Wardell, J. L. In *Comprehensive Organometallic Chemistry*; Wilkinson, G., Stone, F. G. A., Abels, F. W., Eds.; Pergamon: New York, 1982; Vol. 1, Chapter 2. Setzer, W. N.; Schleyer, P. v. R. *Adv. Organomet. Chem.* **1985**, *24*, 354.

(17) Collum, D. B. *Acc. Chem. Res.* **1992**, *25*, 448.

(18) For leading references to rate studies revealing the role of both aggregation *and* solvation see ref 3d.

(19) Newcomb, M. A.; Burchill, M. T. *J. Am. Chem. Soc.* **1984**, *106*, 8276. Streitwieser, A., Jr.; Padgett, W. M., II. *J. Phys. Chem.* **1964**, *68*, 2916. Huisgen, R. In *Organometallic Chemistry*; American Chemical Society: Washington, D. C., 1960, Monograph Series No. 147, pp 36–87. Tobia, D.; Rickborn, B. *J. Org. Chem.* **1989**, *54*, 777.

(20) Williard, P. G.; Liu, Q.-Y. *J. Am. Chem. Soc.* **1993**, *115*, 3380. For related structures see: Stalke, D.; Klingebiel, U.; Sheldrick G. M. *J. Organomet. Chem.* **1988**, *344*, 37. Dipple, K.; Klingebiel, U.; Kottke, T.; Pauer, F.; Sheldrick, G. M.; Stalke, D. *Chem. Ber.* **1990**, *123*, 237.

(21) Matsuda, H.; Hamatani, T.; Matsubara, S.; Schlosser, M. *Tetrahedron* **1988**, *4*, 2865. See also: Schlosser, M.; An, T. D. *Angew Chem., Int. Ed. Engl.* **1981**, *20*, 1039. Schlosser, M.; Tarchini, C.; An, T. D.; Ruzziconi, R.; Bauer, P. J. *Angew Chem., Int. Ed. Engl.* **1981**, *20*, 1041.

(22) Kaufmann, E.; Schleyer, P. v. R.; Houk, K. N.; Wu, Y.-D. *J. Am. Chem. Soc.* **1985**, *107*, 5560. Williard, P. G.; Liu, Q.-Y. *J. Am. Chem. Soc.* **1993**, *115*, 3380. Bernardi, A.; Capelli, A. M.; Cassinari, A.; Comotti, A.; Gennari, C.; Scolastico, C. *J. Org. Chem.* **1992**, *57*, 7029. Bernardi, F.; Bongini, A.; Cainelli, G.; Robb, M.; Valli, G. S. *J. Org. Chem.* **1993**, *58*, 750. Nakamura, E.; Nakamura, M.; Koga, N.; Morokuma, K. *J. Am. Chem. Soc.* **1993**, *115*, 11016. Petasis, N. A.; Teets, K. A. *J. Am. Chem. Soc.* **1992**, *114*, 10328.

nometallic chemistry.[23] Within organolithium chemistry, chelation has been suggested to afford strong metal−ligand bonds and consequent decreased organolithium aggregation states.[16,24] The chelate effect has also been suggested to be the source of substantial perturbations in reactivity and selectivity when a substrate bears the capacity to form a chelated precomplex (referred to as "chelation control" or the "complex-induced proximity effect").[11] A logical synthesis of these two ideas is that a bidentate substrate−lithium interaction could accelerate metalation by facilitating the intervention of monomeric reactive intermediates. Cyclohexanone imines bearing potentially chelating ancillary ligands (**20**) display dichotomous behavior.[3c,d] LDA-mediated metalations in THF proceed by the monomer-based pathway akin to the simple *N*-alkyl derivatives with the pendant ligand playing no measurable role. However, an extremely efficient pathway involving double solvent dissociation via open dimer intermediate **21** dominates in poorly coordinating NR_3 solvents.[3c,d] Although chelates such as **22** based upon monomeric LDA seem equally plausible, they have yet to receive experimental support. The geometries and relative stabilities of the transition structures corresponding to **21** and **22** would help us understand the kinetic consequences of the chelate effect.

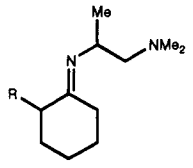

20

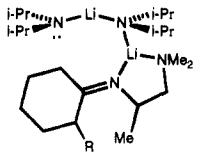

21

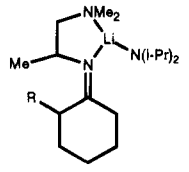

22

The "*Syn* Effect". In the context of imine metalations, the "*syn* effect" refers somewhat loosely to any one of the following:[25] (1) a kinetic preference of imines to metalate the acidic methylene adjacent to (i.e. *syn* to) the *N*-alkyl substituent, (2) a thermodynamic preference of the resulting lithioimines to orient the *N*-alkyl moiety *syn* to the carbanionic carbon, or (3) the kinetic preference of lithioimines to react with electrophiles so as to afford products with the newly introduced substituent and the *N*-alkyl moieties *syn* to each other. The vagueness stems from the widely varying experimental protocols employed to study the *syn*−*anti* preferences—protocols that may or may not address the same phenomena. Early studies led to the suggestion that kinetic metalations occur *anti* to the *N*-alkyl substituent followed by a rapid equilibration and alkylation of *syn*-oriented carbanion to give *syn* products (eq 1).[26] This hypothesis was

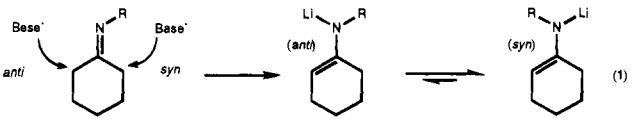

challenged by Bergbreiter and Newcomb and replaced with a model based upon a nonselective kinetic metalation, slow isomerization to *syn*-oriented carbanion, and subsequent *syn* alkylation.[27] During the course of structural studies of lithiated imines,[28] we observed two spectroscopically distinct forms that seemed akin to those assigned by Fraser and co-workers as *syn*

Scheme 1

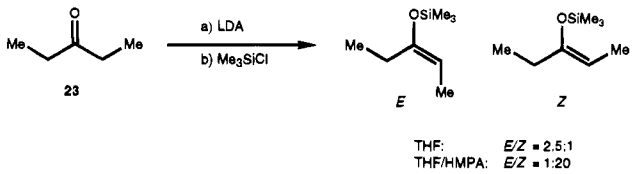

and *anti* isomers,[29] but proved to be stereoisomeric lithioimine dimers. We expressed the concern that lithioimine reactant structures are not necessarily *syn* or *anti*, but otherwise refrained from further comment. Although we were not interested in becoming embroiled in this debate, computational investigations of imine metalations mandated addressing the kinetic *syn* effect.

***E*/*Z* Enolization Selectivities.** A particularly engaging issue concerns the stereoselectivity of enolization of acyclic ketones. In the seminal observation, Ireland and co-workers[30a] reported that LDA-mediated lithiation of 3-pentanone (**23**) in THF affords predominantly the *E* enolate, while added HMPA reverses this preference (Scheme 1). A chairlike transition structure **24** is often invoked to explain the *E* selectivity. Despite some

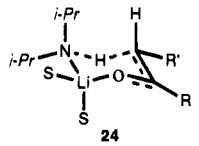

24

suggestions of competing equilibrations as the source of the *Z* selectivities with added HMPA, they also appear to arise from kinetically controlled pathways.[31] Enolizations of 3-pentanone have offered benchmark selectivities for probing lithium amide structure−reactivity relationships and for theory−experiment correlations.[30b,31] Although Narula challenged the chair transition state model[32] and received some support from *ab initio* calculations,[33] the chair model maintains wide popularity. Recent evidence of extreme mechanistic complexity due to the intervention of mixed aggregates clouds the issue.[4,15] Nonetheless, the *E*/*Z* enolization selectivities provide excellent op-

(23) Cotton, F. A.; Wilkinson, G. *Advanced Inorganic Chemistry*, 4th ed.; Wiley: New York, 1980; p 71.

(24) Klumpp, G. W. *Rec. Trav. Chim. Pays-Bas.* **1986**, *105*, 1. *Polyamine-Chelated Alkali Metal Compounds*; Langer, A. W., Jr., Ed.; American Chemical Society: Washington, D.C., 1974.

(25) Fraser, R. R. In *Comprehensive Carbanion Chemistry*; Buncel, E., Durst, T., Eds.; Elsevier: New York, 1980.

(26) Jung, M. E.; Blair, P. A.; Lowe, J. A. *Tetrahedron Lett.* **1976**, *41*, 1439.

(27) Smith, J. K.; Bergbreiter, D. E.; Newcomb, M. *J. Org. Chem.* **1981**, *46*, 3157. Ludwig, J. W.; Newcomb, M.; Bergbreiter, D. E. *J. Org. Chem.* **1980**, *45*, 4666. Lee, J. Y.; Lynch, T. J.; Mao, D. T.; Bergbreiter, D. E.; Newcomb, M. *J. Am. Chem. Soc.* **1981**, *103*, 6215.

(28) Kallman, N.; Collum, D. B. *J. Am. Chem. Soc.* **1987**, *109*, 7466. Wanat, R. A.; Collum, D. B.; Van Duyne, G.; Clardy, J.; DePue, R. T. *J. Am. Chem. Soc.* **1986**, *108*, 3416.

(29) Fraser, R. R.; Chuaqui-Offermanns, N.; Houk, K. N.; Rondan, N. G. *J. Organomet. Chem.* **1981**, *206*, 131.

(30) (a) Ireland, R. E.; Mueller, R. H.; Willard, A. K. *J. Am. Chem. Soc.* **1976**, *98*, 2868. (b) For additional studies of *E*/*Z* enolization selectivities see: Moreland, D. W.; Dauben, W. G. *J. Am. Chem. Soc.* **1985**, *107*, 2264. Corey, E. J.; Gross, A. W. *Tetrahedron Lett.* **1984**, *25*, 491, 495. Prieto, J. A.; Suarez, J.; Larson, G. L. *Synth. Commun.* **1988**, *18*, 253. Masamune, S.; Ellingboe, J. W.; Choy, W. *J. Am. Chem. Soc.* **1982**, *104*, 5526. Gaudemar, M.; Bellassoued, M. *Tetrahedron Lett.* **1989**, *30*, 2779. Kleschick, W. A.; Buse, C. T.; Heathcock, C. H. *J. Am. Chem. Soc.* **1977**, *99*, 247. Heathcock, C. H.; Buse, C. T.; Kleschick, W. A.; Pirrung, M. C.; Sohn, J. E.; Lampe, J. *J. Org. Chem.* **1980**, *45*, 1066. Abdel-Magid, A.; Pridgen, L. N.; Eggleston, D. S.; Lantos, I. *J. Am. Chem. Soc.* **1986**, *108*, 4595. Evans, D. A.; Bartroli, J.; Shih, T. L. *J. Am. Chem. Soc.* **1981**, *103*, 2127. House, H. O.; Czuba, L. J.; Gall, M.; Olmstead, H. D. *J. Org. Chem.* **1969**, *34*, 2324. McCarthy, P. A.; Kageyama, M. *J. Org. Chem.* **1987**, *52*, 4681. Davis, F. A.; Sheppard, A. C.; Chen, B.-C.; Haque, M. S. *J. Am. Chem. Soc.* **1990**, *112*, 6679. Welch, J. T.; Plummer, J. S.; Chou, T.-S. *J. Org. Chem.* **1991**, *56*, 353. Fataftah, Z. A.; Kopka, I. E.; Rathke, M. W. *J. Am. Chem. Soc.* **1980**, *102*, 3959. Nakamura, E.; Hashimoto, K.; Kuwajima, I. *Tetrahedron Lett.* **1978**, *24*, 2079.

(31) Xie, L.; Saunders, W. H., Jr. *J. Am. Chem. Soc.* **1991**, *113*, 3123. Beutelman, H. P.; Xie, L.; Saunders, W. H., Jr. *J. Org. Chem.* **1989**, *54*, 1703. Miller, D. J.; Saunders, W. H., Jr. *J. Org. Chem.* **1982**, *47*, 5039. Beutelman, H. P.; Xie, L.; Miller, D. J.; Saunders, W. H., Jr. *J. Org. Chem.* **1988**, *53*, 2396.

(32) Narula, A. S. *Tetrahedron Lett.* **1981**, *27*, 4119.

Table 1. Transition Structure Enthalpies (H_f) and Activation Enthalpies ($\Delta H^{\ddagger}$) for Cyclic Monomer- and Open Dimer-Based Ketone Metalations (Scheme 2)

entry	amide/substrate/solvent	$H_{f(\text{monomer})}$	$H_{f(\text{open dimer})}$	$\Delta H^{\ddagger}_{(\text{monomer})}$[a]	$\Delta H^{\ddagger}_{(\text{open dimer})}$[a]	$\Delta\Delta H^{\ddagger}$[b]
1	$LiNH_2$/**1**/H_2O	−104.30	−139.10	34.5	35.2	0.7
2	$LiNMe_2$/**2**/H_2O	−115.80	−157.11	37.8	39.7	1.9
3	$LiNMe_2$/**2**/Me_2O	−102.56	−143.35	37.2	35.7	−1.5
4	LDA/**2**/H_2O	−127.07	−178.00	34.2	34.2	0.0
5	LDA/**2**/Me_2O	−112.34	−162.74	31.8	24.8	−7.0
6	LDA/**2**/THF	−120.66	−170.79	31.8	25.4	−6.4
7	LDA/**2**/NMe_3	−62.92	−112.00	26.6	14.7	−11.9
8	LDA/**2**/HMPA	−101.88	−151.53	27.4	23.4	−4.0
9	LDA/**3**/H_2O	−126.30	−175.18	34.8	36.9	2.1
10	LDA/**3**/Me_2O	−111.71	−159.68	32.2	27.7	−4.5
11	LDA/**3**/THF	−120.01	−168.05	32.4	28.1	−4.3
12	LDA/**3**/NMe_3	−61.93	−108.24	27.4	18.4	−9.0
13	LDA/**3**/HMPA	−101.02	−147.92	28.2	26.9	−1.3
14	LDA/**23**/H_2O	−136.09[c]	−182.98[c]	34.4	38.4	4.0
15	LDA/**23**/Me_2O	−121.6[c]	−167.71[c]	31.6	29.0	−2.6
16	LDA/**23**/THF	−129.88[c]	−175.47[c]	31.8	29.9	−1.9
17	LDA/**23**/NMe_3	−72.03[c]	−116.71[c]	26.6	19.2	−7.4
18	LDA/**23**/HMPA	−111.01[c]	−156.25[c]	27.5	27.8	0.3

[a] Activation enthalpies (kcal/mol) are relative to the disolvated cyclic dimer (**25**) and uncoordinated substrate in the most stable conformation. The heats of formation of solvents, substrates, and lithium amide dimers (**25**)[8] (kcal/mol) are as follows: H_2O, −60.9; Me_2O, −51.2; THF, −59.3; NMe_3, −2.8; HMPA, −34.4; **1**, −42.3; **2**, −49.4; **3**, −49.3; $(H_2NLi{\cdot}H_2O)_2$, −193.0; $(Me_2NLi{\cdot}H_2O)_2$, −208.3; $(Me_2NLi{\cdot}Me_2O)_2$, −180.9; $(i\text{-}Pr_2NLi{\cdot}H_2O)_2$, −223.7; $(i\text{-}Pr_2NLi{\cdot}Me_2O)_2$, −189.3; $(i\text{-}Pr_2NLi{\cdot}THF)_2$, −206.1; $(i\text{-}Pr_2NLi{\cdot}NMe_3)_2$, −80.1; $(i\text{-}Pr_2NLi{\cdot}HMPA)_2$, −159.9. [b] $\Delta\Delta H^{\ddagger} = \Delta H^{\ddagger}_{(\text{open dimer})} - \Delta H^{\ddagger}_{(\text{monomer})}$. [c] Heats correspond to most stable (*E*-selective) transition structure. The heats for the *Z*-selective transition structures are available from the data in Table 5.

Scheme 2

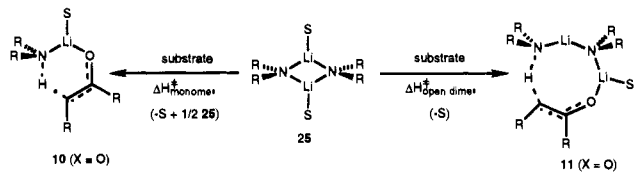

portunities to evaluate the predictive capabilities of computational methods.

Methods.[34] MNDO calculations were performed on an IBM 3090 supercomputer using the MOPAC[35] program with lithium parameters generated by Clark and Theil.[36] All transition structures were fully optimized using the nllsq minimizer and reactant structures with the default minimizer, both under the more rigorous criteria of the keyword PRECISE with no constraints. Maxima were characterized as first order transition structures by normal mode analysis yielding a single imaginary frequency. Internal reaction coordinate (IRC) calculations[37] on selected cases verified that the transition structures correspond to deprotonation reaction coordinates. All transition structures were confirmed to be lacking inordinately short carbon−lithium and hydrogen−lithium contacts that can cause anomalous stabilization.[38]

MNDO calculations provide gas phase enthalpies at 25 °C. The solution and gas phase activation enthalpies are related according to eq 2. The absence of heats of vaporization data renders a quantitative theory−experiment comparison impossible. Nevertheless, the method's reliability has been clearly established for ground state computations of organolithium compounds in general and lithium amides in particular.[7-9] Additionally, it is often not constructive to compare free energies of activation for reactions of different molecularities (whether calculated or measured) due to the standard state dependence of the translational entropy component. The calculations are referenced to solvent (i.e. ligand), substrate, and reagent concentrations of 1.0 molar—conditions rarely maintained experimentally. Since lower base concentrations and higher solvent concentrations will promote reaction via the more highly solvated and less aggregated monomer transition structure, the enthalpy calculations offer a lower bound for contribution of the monomer pathway. Furthermore, investigations of the solvents' and substituents' impact on the relative activation enthalpies ($\Delta\Delta H^{\ddagger}$) eliminate the mass action considerations.

$$\Delta H^{\ddagger}(\text{solution}) = \Delta H^{\ddagger}(\text{gas}) - \Sigma\Delta H(\text{vaporization}) \quad (2)$$

Since MNDO does not optimize core orbitals, dynamical electron correlation error will be present. Nondynamical electron correlation error resulting from the topography of the potential energy surface (i.e. breaking bonds) should also be present. The utility of MNDO relies heavily upon the extent to which dynamical (structure-independent) and nondynamical (structure-dependent) electron correlation errors in the reactant and transition structure cancel.[39] The capacity of any molecular orbital package based upon single-determinant wave functions to treat both aspects of the potential energy surface with consistency is questionable. Furthermore, electron correlation is included implicitly to an unknown extent in the MNDO parameters. It has been suggested that MNDO underestimates activation barriers by approximately 10 kcal/mol in the absence of additional corrections for electron correlation.[40] Nevertheless, such systematic errors are more likely to cancel by considering *relative* barrier heights.

Results

The results are organized according to three general substrate classes (**1**−**3**, **4**−**6**, and **7**−**9**, Chart 1) and two distinct pathways based upon monomer and open dimer transition structures (**10** and **11**, Chart 2). We will begin with general descriptions of the key geometric attributes of the monomer and open dimer transition structures. Descriptions of geometries will be followed by discussions of the deprotonation activation enthalpies, emphasizing the consequences of increasing steric demands of the R_2NLi base, solvent, and substrate. References to lithium amide/solvent combinations (e.g. $LiNH_2/H_2O$ or LDA/Me_2O) connote the disolvated cyclic dimer ground states (**25**). Absolute

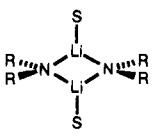

25

Table 2. Transition Structure Enthalpies (H_f) and Activation Enthalpies ($\Delta H^{\ddagger}$) for Cyclic Monomer- and Open Dimer-Based *N*-Alkylimine Metalations (Scheme 3)

entry	amide/substrate/solvent	$H_{f(\text{monomer})}$	$H_{f(\text{open dimer})}$	$\Delta H^{\ddagger}_{(\text{monomer})}$[a]	$\Delta H^{\ddagger}_{(\text{open dimer})}$[a]	$\Delta\Delta H^{\ddagger}$[b]
1	$LiNH_2$/**4**/H_2O	−55.12	−90.56	32.5	32.6	0.2
2	$LiNMe_2$/**5a**/H_2O	−66.75	−106.11	37.1	41.0	3.9
3	$LiNMe_2$/**5a**/Me_2O	−53.64	−92.48	36.5	36.9	0.4
4	LDA/**5a**/H_2O	−78.64	−122.20	32.9	40.3	7.4
5	LDA/**5a**/Me_2O	−64.23	−106.76	30.1	31.0	0.9
6	LDA/**5a**/THF	−72.28	−114.76	30.5	31.7	1.3
7	LDA/**5a**/NMe_3	−12.71	−52.18	27.0	24.8	−2.2
8	LDA/**5a**/HMPA	−50.86	−92.96	28.8	32.2	3.4
9	LDA/**5b**/H_2O	−78.64[c]	−123.74[c]	38.8	44.7	5.9
10	LDA/**5b**/Me_2O	−64.23[c]	−106.89[c]	36.0	36.8	0.8
11	LDA/**5b**/THF	−72.28[c]	−114.43[c]	36.4	38.0	1.6
12	LDA/**5b**/NMe_3	12.57[c]	−49.77[c]	33.1	33.2	0.1
13	LDA/**5b**/HMPA	−50.94[c]	−92.39[c]	34.6	38.7	4.1
14	LDA/**6**/H_2O	−63.21	−108.13	55.6	61.6	6.0
15	LDA/**6**/Me_2O	−48.50	−91.82	53.1	53.2	0.1
16	LDA/**6**/THF	−56.58	[d]	53.4	–	–
17	LDA/**6**/NMe_3	3.48	[d]	50.4	–	–
18	LDA/**6**/HMPA	−35.32	[d]	51.5	–	–

[a] Activation energies (kcal/mol) correspond to the *anti* forms and are scaled relative to the disolvated cyclic dimer (**25**) and uncoordinated substrate in the most stable conformation. The heats of formation of solvents and lithium amide dimers are listed in Table 1 caption. The heats of formation of substrates (kcal/mol) are as follows: **4**, 8.9; **5a**, 0.3; **5b**, −5.6; **6**, −6.9. [b] $\Delta\Delta H^{\ddagger} = \Delta H^{\ddagger}$(open dimer) − $\Delta H^{\ddagger}$(monomer). [c] Corresponds to *anti* transition structures. [d] No first order transition structures located with retention of solvent.

Scheme 3

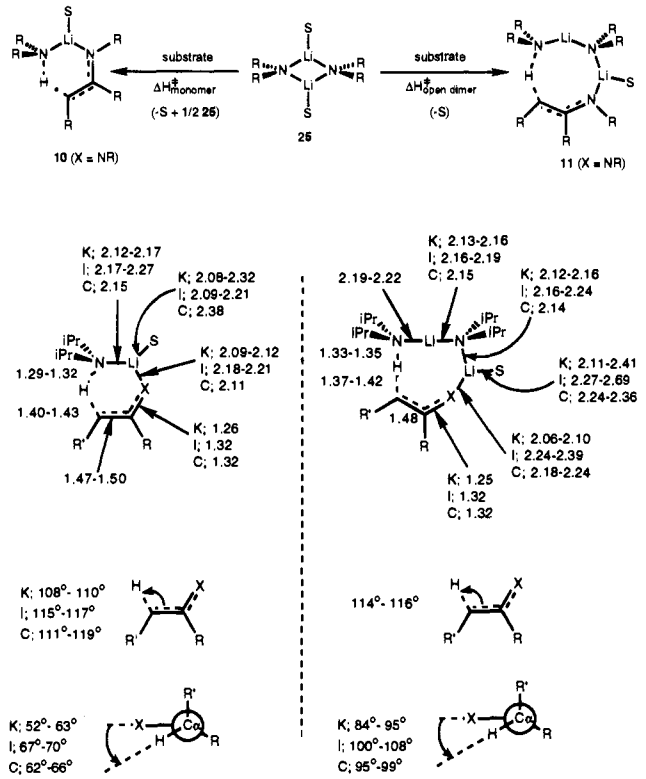

Figure 1. Summary of selected bond distances, bond angles, and torsional angles found in cyclic monomer- and open dimer-based transition structures for LDA-mediated metalations. All distances are reported in Å. Values specific to ketones, *N*-alkylimines (*anti* forms), or chelating imines are denoted with prefixes K, I, and C (respectively), while unlabeled values are common to all substrates. Values are listed either as ranges or as averages of especially narrow ranges.

heats of formation (H_f) of the lithium amide reactants have been reported previously and are listed in the caption of Table 1.[8] The absolute heats of formation of the reactant and transition structures are included in Tables 1−3 along with the metalation activation enthalpies for specific base/solvent/substrate combinations. Heats of solvent substitution of LDA reactant and metalation transition structures are compiled in Table 4. *E*/*Z* selectivities for 3-pentanone enolizations are listed in Table 5.

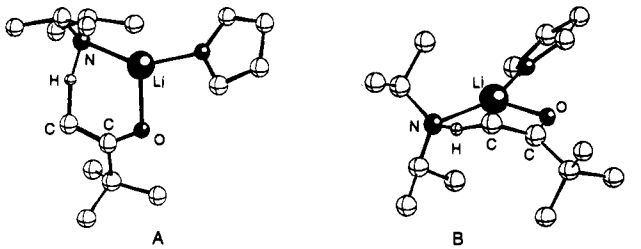

Figure 2. LDA/3/THF transition structure for monomer-based enolization. Hydrogens other than the abstracted proton are omitted for clarity. (A) View normal to approximate plane of ring. (B) View from side of ring.

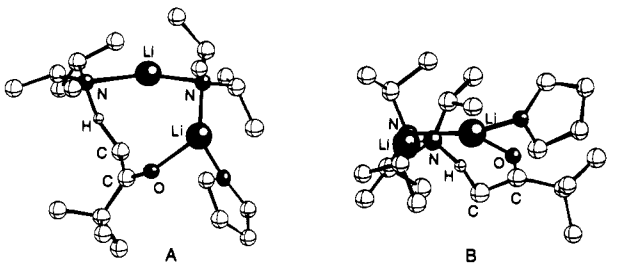

Figure 3. LDA/3/THF transition structure for open dimer-based enolization. Hydrogens other than the abstractd proton are omitted for clarity. (A) View normal to approximate plane of ring. (B) View from side of ring.

Relative energies of *syn* and *anti* transition structures for *N*-alkylimine metalations are listed in Table 6.

Ketone Metalations: Transition Structure Geometries. The geometries of both monomer and open dimer transition structures are remarkably consistent among the various lithium amide/substrate/solvent combinations. Geometries of the monomeric transition structures are shown in Figures 1 and 2. Internal angles within the ring vary by less than 5°. The six-membered rings bear little resemblance to standard cyclohexane conformations. The ring of the unhindered $LiNH_2$/acetaldehyde/H_2O transition structure displays a puckering along the axis between the lithium and the acidic carbon that is unique to the minimally substituted system. The puckered structure resembles the unsolvated $LiNH_2$/acetaldehyde structure calculated with *ab initio* methods by McKee[41] and Houk.[33] Inclusion of alkyl groups on the lithium amide, substrate, and solvent fragments

Table 3. Transition Structure Enthalpies (H_f) and Activation Enthalpies ($\Delta H^{\ddagger}$) for Cyclic Monomer- and Open Dimer-Based Chelating Imine Metalations (Scheme 4)

entry	amide/substrate/solvent	$H_{f(\text{monomer})}$[a]	$H_{f(\text{open dimer})}$[a]	$\Delta H^{\ddagger}_{(\text{monomer})}$[b]	$\Delta H^{\ddagger}_{(\text{open dimer})}$[b]	$\Delta\Delta H^{\ddagger}$[c]
1	$LiNH_2$/**7**/H_2O	9.05	−27.13	38.9	38.3	0.6
2	$LiNMe_2$/**8**/H_2O	9.51	−32.17	43.0	44,5	1.6
3	$LiNMe_2$/**8**/Me_2O	−1.06	−49.51	39.0	36.5	−2.4
4	LDA/**8**/H_2O	−1.06	−49.51	40.1	42.6	2.5
5	LDA/**8**/Me_2O	−1.06	−49.51	32.6	27.6	−5.0
6	LDA/**8**/THF	−1.06	−49.51	32.9	28.2	−4.7
7	LDA/**8**/NMe_3	−1.06	−49.51	26.4	15.2	−11.2
8	LDA/**8**/HMPA	−1.06	−49.51	34.7	31.8	−2.9
9	LDA/**9a**/H_2O	7.30	−36.67	50.6	57.6	7.0
10	LDA/**9a**/Me_2O	7.30	−36.67	43.6	42.6	−0.5
11	LDA/**9a**/THF	7.30	−36.67	43.4	43.2	−0.2
12	LDA/**9a**/NMe_3	7.30	−36.67	37.0	30.3	−6.7
13	LDA/**9a**/HMPA	7.30	−36.67	45.2	46.8	1.6
14	LDA/**9b**/H_2O	10.73	−31.12	54.3	63.4	9.1
15	LDA/**9b**/Me_2O	10.73	−31.12	46.8	48.4	1.6
16	LDA/**9b**/THF	10.73	−31.12	47.1	49.0	1.9
17	LDA/**9b**/NMe_3	10.73	−31.12	40.6	36.1	−4.6
18	LDA/**9b**/HMPA	10.73	−31.12	48.9	52.6	3.7

[a] Common heats for different solvents stem from the complete desolvation (see text). [b] Activation energies (kcal/mol) are relative to the disolvated cyclic dimer (**25**) and uncoordinated substrate in the most stable conformation. The heats of formation of solvents and lithium amide dimers are listed in Table 1 caption. The heats of formation of substrates (kcal/mol) are as follows: **7**, 5.8; **8**, 9.8; **9a**, 7.6; **9b**, 7.4. [c] $\Delta\Delta H^{\ddagger} = \Delta H^{\ddagger}$(open dimer) − $\Delta H^{\ddagger}$(monomer).

Scheme 4

causes flattening of the ring to near planarity for LDA-based transition structures solvated by the bulkier ethereal and amine solvents (Figure 2). The 52−63° HCCO torsion angles may represent a compromise between stereoelectronic preferences for alignment with the carbonyl group and constraints imparted by the ring structure. The most substantial deviations from the ideal 90° HCCO torsion angle[42,43] are observed with sterically demanding lithium amide/solvent/substrate combinations. The C−O and C−C bond lengths differ only slightly from those observed in the starting carbonyl substrates. The N−H−C angles show little variation (≈160°) and are in fair accord with Narula's model of linear proton transfer.[32]

The open dimer transition structures (Figures 1 and 3) share several geometrical characteristics with ground state open dimers[8,20] and bear little semblance to standard carbocyclic eight-membered rings.[42,44] The ring forms a smooth loop that positions the lone pair-bearing nitrogen proximate to the acidic proton. The fundamental geometry of the eight-membered ring varies only marginally with changes in the lithium amide, substrate, or solvent. The lithium amide *N*-alkyl groups show some rotation away from being coplanar, presumably to avoid steric interactions. The internal N−Li−N angles approach linearity (≈155°) as found in ground state lithium amide open dimers.[8] The 163−165° N−H−C angle is more nearly linear

Table 4. Heats of Solvent Substitution (ΔH) of the Cyclic Transition Structures for LDA-Mediated Metalation (Scheme 5)[a]

		substrate			
solvent	mechanism	**2**	**3**	**5b**	**6**
NMe_3	monomer	1.3	1.6	2.4	3.6
	open dimer	2.3	3.3	8.1	[b]
HMPA	monomer	−6.1	−5.9	−3.5	−3.6
	open dimer	−5.6	−4.8	−2.9	[b]

[a] Entries correspond to enthalpies of substitution (ΔH, kcal/mol) according to Scheme 5. The corresponding substitutions of THF from the LDA reactant (**25**) by NMe_3 and HMPA are 13.0 and −3.6 kcal/mol, respectively. [b] No first order transition structures found.

Scheme 5

than in the monomer transition structures. The torsion angles about the HCCO atoms are consistently close to 90°. Both angles are indicative of a greater flexibility of the open dimer to achieve the stereoelectronically most favorable deprotonation

(33) Houk and Li calculated the cyclic transition structures for the metalation of acetaldehyde by $LiNH_2$ using partial optimization with a 3-21G basis set with subsequent single point energy determination with higher (6-31G* and 6-31+G*) basis sets. They also described calculations of propionaldehyde metalation by cyanide ion via *acyclic* transition structures that revealed a *Z* selectivity. Houk, K. N.; Li, Y. Personal communication.

(34) For general discussions of transition structure optimizations, see: Bernardi, F.; Robb, M. A. *Adv. Chem. Phys.* **1987**, *67*, 155. Schlegel, H. B. *Adv. Chem. Phys.* **1987**, *67*, 249.

(35) Stewart, J. J. P. *QCPE*, 581.

(36) Clark, T. and Thiel, W. T. *QCPE*, 438.

(37) Schmidt, M. W.; Gordon, M. S.; Dupuis, M. *J. Am. Chem. Soc.* **1985**, *107*, 2585.

(38) Glaser, R.; Streitwieser, A., Jr. *THEOCHEM* **1988**, *163*, 19.

(39) Sinanoglu, O.; Bruckner, K. A. *Three Approaches to Electron Correlation in Molecules*; Yale Univ. Press: New Haven, 1970.

(40) Theil, W. T. *Tetrahedron* **1988**, *44*, 24.

(41) McKee, M. L. *J. Am. Chem. Soc.* **1987**, *109*, 559.

(42) Nasipuri, D. In *Stereochemistry of Organic Compounds*; Wiley: New York, 1991; p 386.

(43) For the original work, see: Corey, E. J. *Experientia* **1953**, *9*, 329. Corey, E. J.; Sneen, R. A. *J. Am. Chem. Soc.* **1956**, *78*, 154.

(44) Hendrickson, J. B. *J. Am. Chem. Soc.* **1967**, *89*, 7036. Juaristi, E. In *Introduction to Stereochemistry and Conformational Analysis*; Wiley: New York, 1991; p 250.

alignment.[45,46] The two alkyl substituents of the ketone substrate are generally free of spatial interactions with the remainder of the transition structure. In the more hindered LDA cases, the solvent bends away from the bulky lithium amide *N*-alkyl groups. The relatively uncongested region about the carbonyl oxygen allows both the solvent and ketone substituents to conformationally relax. This represents an important distinction between ketone enolizations and imine metalations (see below).

The one crystal structure of a lithium amide open dimer reveals longer (dimer-like) LiN−LiN and shorter (monomer-like) LiNLi−N distances[20] that correlate with bond lengths calculated by MNDO[8] and appear to correlate with $^{6}Li-^{15}N$ one-bond coupling constants.[6] The minimally substituted $LiNH_2$/acetaldehyde/H_2O or $LiNMe_2$/acetone/H_2O transition structures display LiN−LiN and LiNLi−N bond lengths that are nearly equal. In contrast, the LDA open dimer transition structures show bond lengths for all solvent/substrate combinations that display short LiNLi−N and long LiN−LiN bonds analogous to those found in the ground state structures. The C−O and C−C bond lengths are equivalent to those calculated in the monomeric structures. The uniformly longer N−H bonds and shorter C−H bonds relative to the monomer transition structures are suggestive of a lesser degree of proton transfer.

Intrinsic reaction coordinate (IRC) calculations were used to verify that (selected) transition structures correspond to deprotonation reaction coordinates.[37] As an interesting aside, the first stable intermediate following the open dimer transition structure proves to be mixed dimer **26**. Such mixed dimers have been the topic of considerable discussion as kinetically important species in the context of ketone enolizations and related reactions of lithium dialkylamides.[3,9,15,47]

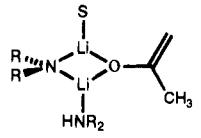

26

Ketone Metalations: Activation Enthalpies. Calculated activation enthalpies for ketone enolizations via monomer and open dimer transition structures (Scheme 2) are listed in Table 1. First looking at the monomer-based pathway, we find that increasing the lithium amide bulk reduces the activation enthalpies. This is consistent with the notion that relief of the high steric congestion in the lithium amide dimers upon proceeding to the transition structure imparts the dialkylamide bases with their high reactivity. Comparison of the activation enthalpies for acetone (**2**) and pinacolone (**3**) metalations reveal an insensitivity to the steric demands of the substrate bulk, consistent with monomeric enolization transition structures that are not very sterically congested. Solvent perturbations show a significant influence on the calculated barriers, with predicted metalation rates following the order: NMe_3 > HMPA > THF ≈ Me_2O > H_2O. Within this series we find an interesting result: monomer-based metalations are predicted to be accelerated (relative to THF) by either the weakly coordinating NMe_3 or strongly coordinating HMPA. NMe_3 and HMPA are both sterically demanding, yet have very different affinities for lithium ion.[8,48] The origins of reduced activation enthalpies caused by NMe_3 and HMPA relative to THF are very different as seen by inspection of the enthalpies of ligand substitution. HMPA imparts stabilization to the transition state that is greater than in the ground state (Table 4). In contrast, NMe_3 is destabilizing in the ground state, yet less so in the transition state. This further reveals a theme that is both recurring and quite important: *the high reactivities of hindered lithium dialkylamides stem from relief of steric demands.*

The open dimer-based enolizations show an enhanced sensitivity to amide steric bulk relative to the monomer cases. The barriers are predicted to increase marginally with the increased ketone bulk (pinacolone vs acetone) for the ethereal solvents, but increase markedly with substrate bulk for the NMe_3 solvated cases where destabilizing solvent/substrate interactions become substantial. The open dimer-based enolization pathways are predicted to display the same solvent-dependent rates as the monomer-based pathways: NMe_3 > HMPA > THF ≈ Me_2O > H_2O. The open dimer transition structures are found to be more strongly stabilized by solvation than the dimeric LDA reactant (Table 4), yet less dramatically than for the monomeric transition structures. The open dimer transition structures appear to be more sterically demanding than the monomer structures. The increased bulk of pinacolone is destabilizing for bulky solvents as seen in the enthalpies of THF substitution by NMe_3 and HMPA (Table 4). However, the desolvation accompanying the open dimer-based metalations magnifies the accelerating effects of the weakly coordinating NMe_3 ligands, yet attenuates the acceleration by HMPA.

We can now consider solvent and substituent effects on the *relative* efficacies of the monomer and open dimer pathways. Within the R_2NLi/H_2O series, increasing the steric demands of the *N*-alkyl substituents on the lithium amide base accelerates the metalation via both pathways (cf. entries 2−4 and 3−5, Table 1), yet more strongly so for the open dimer mechanism (cf. R_2NLi/Me_2O/acetone metalations; cf. entries 2−4 and 3−5). Conversely, with the bulky lithium amides, an increase in the steric demands of the solvent accelerates both pathways, disproportionately so for the open dimer pathway (cf. acetaldehyde metalations by R_2NLi/H_2O and R_2NLi/Me_2O in entries 2/3, 4/5, and 9/10). Overall, MNDO predicts a relative promotion of open dimer-based metalations with increasing amide and solvent steric demands. However, we caution against adopting an oversimplified model of solvation effects; these relative monomer and open dimer activation enthalpies derive from a complex interplay of reactant and transition structure stabilities. The influence of substrate on the relative monomer and open dimer enolization rates is seen by comparing LDA-mediated metalations of acetone (Table 1; entries 4−8) and pinacolone (entries 9−13). Although the open dimer mechanism is predicted to dominate under all circumstances, increased substrate bulk renders the monomer mechanism increasingly competitive. This would seem to suggest that monosolvated open dimer transition structures (e.g. **11**) are more sensitive to substrate steric demands than the monosolvated monomer transition structures (e.g. **10**).

Ketone Metalations: *E/Z* Selectivities. We explored the enolization of 3-pentanone by LDA (Scheme 1) to ascertain

(45) Beckwith, A. L. J.; Ingold, K. U. In *Rearrangements in Ground and Excited States*; Academic Press: New York, 1980; p 251. Bigeliesen, J. *Pure Appl. Chem.* **1964**, *8*, 217. Albery, W. J. *Trans. Farad. Soc.* **1967**, *63*, 200. Bell, R. P. *The Proton in Chemistry*; Cornell University Press: Ithaca, 1973.

(46) Internal deprotonations have been suggested to be optimal for eight-membered rings: McManus, S. P.; Capon, B. *Neighboring Group Participation*; Plenum Press: New York, 1976, p 58. See also: Bernardi, A.; Capelli, A. M.; Cassinari, A.; Comotti, A.; Gennari, C.; Scolastico, C. *J. Org. Chem.* **1992**, *57*, 7029. Bernardi, F.; Bongini, A.; Cainelli, G.; Robb, M.; Valli, G. S. *J. Org. Chem.* **1993**, *58*, 750.

(47) Williard, P. G.; Liu, Q.-Y. Unpublished.

(48) For a discussion of the cone angle of trialkylamines in the context of transition metal ligation see: Seligson, A. L.; Trogler, W. C. *J. Am. Chem. Soc.* **1991**, *113*, 2520.

Table 5. Predicted Relative Activation Enthalpies for LDA-Mediated 3-Pentanone (**23**) Enolizations ($\Delta\Delta H^{\ddagger}E/Z$,[a] kcal/mol)[b]

	transition structure				
solvent	**10**	**11**	**12**	**13**	**14**
H_2O	−0.2	−0.5	−3.4	1.4	2.0[c]
Me_2O	−0.5	−0.6	0.2	1.2	2.0[c]
THF	−0.4	−0.4	2.0	1.4	2.0[c]
NMe_3	−0.9	−0.7	[d]	[d]	2.0[c]
HMPA	−1.0	−0.6	0.5	0.7	2.0[c]

[a] $\Delta\Delta H^{\ddagger}_{E/Z} = \Delta H^{\ddagger}_{E} - \Delta H^{\ddagger}_{Z}$ (see Scheme 1). [b] The calculated heat of formation of 3-pentanone is −58.6 kcal/mol. [c] Calculated without including the $+LiS_4$ counterion. [d] Not calculated.

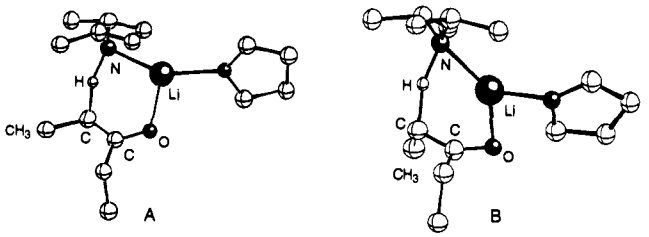

Figure 4. LDA/**23**/THF transition structures for monomer-based enolizations: (A) *E*-selective; (B) *Z*-selective. Hydrogens other than the abstracted proton are omitted for clarity.

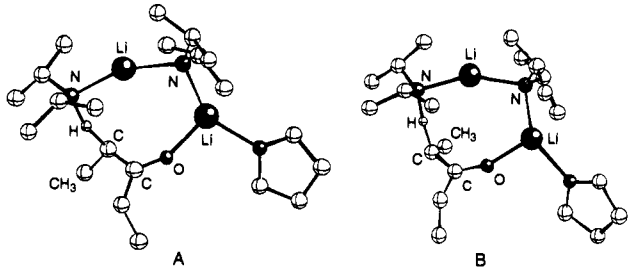

Figure 5. LDA/**23**/THF transition structure for open dimer-based enolizations: (A) *E*-selective; (B) *Z*-selective. Hydrogens other than the abstracted proton are omitted for clarity.

the origins of the solvent-dependent *E*/*Z* selectivities (Table 5; Figures 4 and 5). For all solvents (including HMPA), both the cyclic monomer and open dimer-based pathways display modest and remarkably invariant *E* selectivities. The *E* selectivity predicted for HMPA contrasts with experiment.[49]

The failure to find possible origins of the *Z*-selective enolizations prompted us to investigate pathways involving acyclic transition structures (corresponding to **12** and **13**). We extended this investigation to include triple ions (e.g. **14**) due to their possible importance under highly ionizing conditions.[50] The activation enthalpies are inordinately high (although less so for HMPA) due to either the chemistry or the computational method. Accordingly, we have limited the discussion to a qualitative description of geometries. The *E*/*Z* selectivities are listed in Table 5. Representative transition structures are illustrated in Figures 6 and 7. Since precomplexation is not involved, the acyclic monomer and open dimer transition structures differ from their cyclic counterparts due to an additional coordinated solvent molecule. The most provocative result is that all three acyclic mechanisms include provisions for *Z*-selective enolizations for all solvents. In addition, the triple ion offered an unanticipated insight into the possible role

(49) Saunders could find no evidence of competing equilibrations during enolizations of 3-pentanone at −78 °C in the absence or presence of HMPA.[31] Our own investigations are in accord with this conclusion: Romesberg, F. E.; Collum, D. B., unpublished.

(50) For a bibliography and further leading references to the role of triple ions in organolithium chemistry see ref 9.

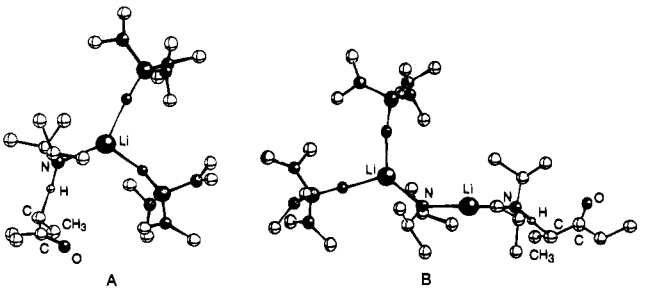

Figure 6. LDA/**23**/HMPA *acyclic* transition structure for *Z*-selective enolizations: (A) monomer-based; (B) open dimer-based. Hydrogens other than the abstracted proton are omitted for clarity.

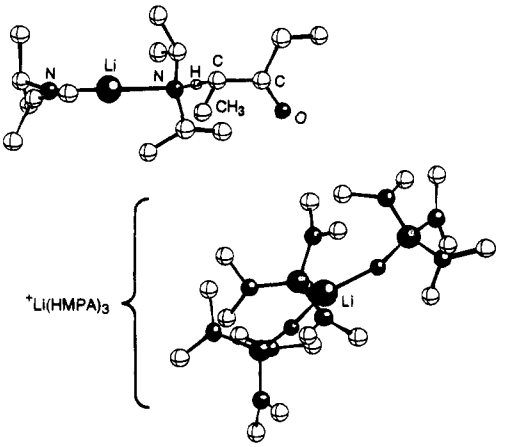

Figure 7. LDA/**23**/HPMA *acyclic* transition structure for *Z*-selective triple ion-based enolization. Hydrogens other than the abstracted proton are omitted for clarity.

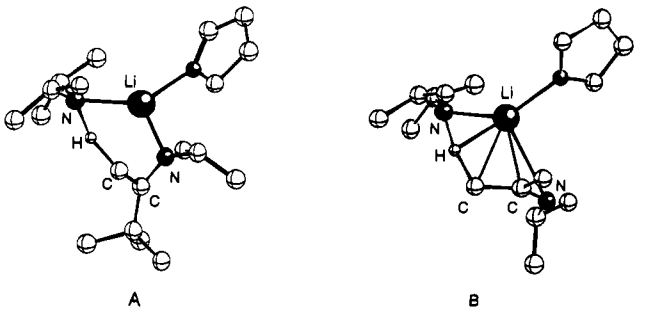

Figure 8. LDA/**6**/THF cyclic monomer-based transition structures: (A) *anti* metalation; (B) *syn* metalation. Hydrogens other than the abstracted proton are omitted for clarity.

of the HMPA-solvated counterion. An extended structure with the lithium counterion oriented away from the N−Li−N fragment is the most stable (Figure 7), yet the counterion position seems relatively unimportant. Interestingly, the lithium counterion shows a preference for a trigonal planar tris solvation state despite a substantial (>6 Å) Li−O contact. The high (36.3 kcal/mol) stabilization by ion pairing does not appear to be due to a conventional Lewis acid−base interaction.

***N*-Alkylimine Metalations: *Syn*−*Anti* Selectivity.** The prominent difference between ketones and imines is the sterically demanding imine *N*-alkyl moiety. We first had to determine the relative tendencies for metalation *syn* and *anti* with respect to the imine *N*-alkyl group. Experimental evidence suggests that both *syn* and *anti* deprotonations are nearly equally viable (eq 1).[27] Indeed, we were able to find *syn* and *anti* transition structures for both the monomer- and open dimer-based transition structures (Figures 8 and 9). Unfortunately, the most stable *syn*-oriented monomer-based structures each show a substantial distortion placing the lithium in close contact

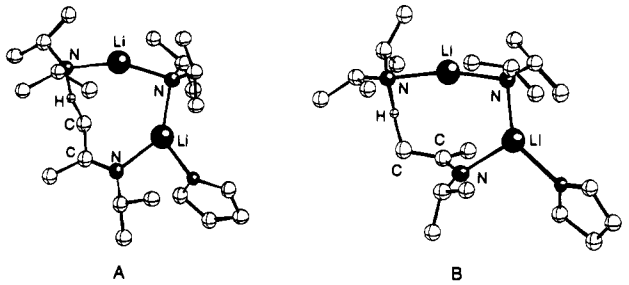

Figure 9. Cyclic monomer-based transition structures: (A) LDA/**6**/THF *anti* metalation; (B) LDA/**5b**/THF *syn* metalation. Hydrogens other than the abstracted proton are omitted for clarity.

Table 6. Predicted *Syn*–*Anti* Relative Activation Enthalpies for LDA-Mediated Metalations of Imine **5b** via Monomer- and Open Dimer-Based Cyclic Transition Structures (Figures 8 and 9)

solvent	$\Delta\Delta H^{\ddagger}_{(monomer)}$[a]	$\Delta\Delta H^{\ddagger}_{(open\ dimer)}$[a]
H_2O	3.2	1.9
Me_2O	4.9	4.0
THF	3.8	3.4
NMe_3	5.1	1.3
HMPA	1.5	2.7

[a] $\Delta\Delta H^{\ddagger} = \Delta H^{\ddagger}_{anti} - \Delta H^{\ddagger}_{syn}$ (kcal/mol; positive value indicates greater *anti* stability). [b] The calculated heats of formation are available from the data in Table 2.

with both $[C{=}CNR]^{\delta-}$ carbons and the acidic proton at the expense of the in-plane N–Li contact (Figure 8b). On the one hand, this π interaction is pleasing to the extent that we had invoked intermediates such as **18** on several occasions; they appeared to be the only plausible structures bearing a monomeric LDA fragment (mandated by the rate equations) within reach of the protons on the *syn* methylene group. On the other hand, it has been suggested that structures bearing close C–Li and H–Li contacts will be anomalously (erroneously) stabilized relative to structures lacking such contacts (such as the *anti* structures, Figure 8a).[38] Thus, while the *syn*-oriented monomer-based structures are only moderately (1–3 kcal/mol) less stable than the *anti*, it is not possible to assess the extent (if any) that the stability of the *syn* structures are overestimated.

The situation for the *syn* open dimer transition structures was somewhat better in that they showed no C–Li or H–Li contacts (Figure 9b). Furthermore, we found it quite provocative that they included sufficient flexibility to allow reasonable alignments for a *syn* metalation with Li π complexation to the two carbons of the $[C{=}CNR]^{\delta-}$ fragment. However, as we shall note in more detail below, the *anti* open dimer structures are generally not favorable for *N*-alkylimine metalations, and the *syn*-oriented open dimers are even less stable than the *anti* open dimers.

Overall, we find no immutable arguments against the chemical plausibility of the *syn*-oriented monomer- or dimer-based systems. However, with direct comparisons of the monomer-based *syn* metalations to the other pathways rendered questionable, we have chosen to base subsequent discussions on the more favorable *anti* structures. Nonetheless, we have archived the relative *syn* and *anti* transition structure stabilities in Table 6.

We also briefly investigated acyclic transition structures for evidence of a *syn* selectivity not found for the cyclic monomer- and open dimer-based reaction pathways. The enthalpies proved to be considerably higher than for the cyclic transition structures, precluding a detailed discussion. However, in much the same way that the acyclic transition structures displayed the elusive provision for *Z*-selective enolizations, they also included provisions for *syn* selective imine metalations; within the relatively high energy acyclic transition structures, the *syn* isomers (see Figure 10) are found to be more stable. These results will be placed in the context of the "*syn effect*" in Discussion.

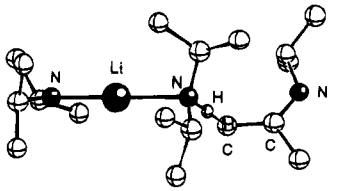

Figure 10. LDA/**5b** acyclic transition for *syn*-selective triple ion-based deprotonation Hydrogens other than the abstracted proton and cation are omitted for clarity.

***N*-Alkylimine Metalations: Transition Structure Geometries.** The structural details of the monomer-based (*anti*) transition structures for imine metalation are generally quite similar to those described above for enolizations (Figures 1 and 8a). The N–H–C deprotonation bond angles are indistinguishable from those found in the enolization structures, while the 67–70° HCCN torsion angles more closely approximate the stereoelectronically preferred 90° value.[42] The solvent is buttressed between the *N*-alkyl groups of the imine and lithium amide moieties. The methyl groups of the *N*-isopropyl substituent orient away from the solvent. The imine monomer transition structures are more nearly planar than the analogous ketone structures. The CCXLi (X = N or O) torsion angle is consistently 14–18° compared to 35–40° for the corresponding enolizations. The difference presumably derives from the buttressing of the solvent with the imine *N*-alkyl groups.

The general ring geometries of the cyclic open dimer transition structures for imine metalations are similar to those described for enolizations; however, slightly elongated C–H bonds and shortened N–H bonds are indicative of more product-like transition structures. The extent of proton transfer appears to be closely matched to the ketone and imine monomer transition structures. The HCCN torsion angles fall within a narrow range of 100–108°. The buttressing of the solvent between lithium amide and substrate *N*-alkyl group is amplified by the increased internal angles of the eight membered ring relative to a six-membered ring transition structure. Imine *N*-isopropyl groups interact with the solvent, causing elongation of solvent–lithium contacts in the least hindered solvent/substrate combinations. The more sterically demanding solvent/substrate combinations fail to afford reasonable transition structures. All optimizations of *N*-isopropylimines of pinacolone solvated by THF, NMe_3, and HMPA afforded transition structures with the solvent extruded.

***N*-Alkylimine Metalations: Activation Enthalpies.** The calculated activation enthalpies for *N*-alkylimine metalations (Scheme 3) are listed in Table 2. As seen in the enolizations, increased lithium amide bulk lowers the activation enthalpies for monomer-based metalations. Importantly, the high steric demands of the imine *N*-alkyl group destabilize the transition structures with consequent increased activation enthalpies. This accounts for the low kinetic acidities of imines relative to ketones. The high sensitivity of the calculated barriers to substrate bulk constitutes additional evidence of increased steric congestion in the imine transition structures relative to those for ketone enolizations and is consistent with experiment.[3] The solvent-dependent metalation rates (following the order NMe_3 > HMPA > THF $\approx$ Me_2O > H_2O) reveal the important recurring theme: monomer-based metalations are accelerated by sterically demanding ligands, whether the ligands are weakly coordinating (NMe_3) or strongly coordinating (HMPA). Inspection of the enthalpies of THF displacement from the dimeric

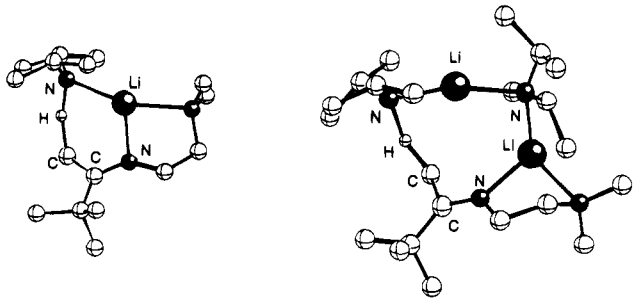

Figure 11. LDA/**9a** transition structure for chelation-assisted deprotonation: (A) monomer-based; (B) open dimer-based. Hydrogens other than the abstracted proton are omitted for clarity.

reactants and monomer-based transition structures (Table 4) reveals the same trend found in the ketone enolizations; HMPA imparts stabilization to the transition state that is greater than in the ground state while NMe_3 is destabilizing in the ground state, yet less so in the transition state. However, the increased bulk of imines relative to ketones attenuates the steric differences between the ground and transition states.

The activation enthalpies of open dimer-based metalations also exhibit high sensitivities to steric effects. Where comparisons are available (imine **5b**), the predicted rate follows the order: NMe_3 > THF ≈ Me_2O > HMPA > H_2O. The open dimer mechanism is accelerated by NMe_3 relative to THF, but less noticeably than in ketones due to the higher steric congestion in the open dimer transition structure. Metalations of the pinacolone-derived imines manifest high barriers relative to the acetone imine. For the most hindered lithium amide/solvent/substrate combinations we were not able to locate stable monosolvated transition structures due to desolvation. (Locking the solvent linkage to prevent desolvation affords inordinately destabilized secondary transition structures.) This offers tacit evidence that the open dimer pathway is sterically very demanding. That is not say, however, that an unsolvated open dimer pathway can be excluded from consideration.

Comparison of the open dimer- and monomer-based metalations reveals nearly equivalent activation enthalpies for the least congested imine metalations (Table 2, entry 1). However, the monomer-based metalations become preferred with increasing steric demands of the solvent (entries 2 and 3) and lithium amide base (entries 4−8). The overall facilitation of the monomer-based mechanism follows the order: H_2O > HMPA > Me_2O ≈ THF > NMe_3. The failure to locate stable THF-, NMe_3-, and HMPA-solvated open dimer transition structures for pinacolone *N*-isopropyl imine metalations seems consistent with the trend toward monomer-based metalations in the most hindered imine substrates.

Chelating Imine Metalations: Transition Structure Geometries. We investigated the influence that potentially chelating *N*-alkyl substituents of imines **7**−**9** would have on the structures and relative energies of the monomer and open dimer transition structures (**15** and **16**, Chart 2). The general geometric attributes for the chelated monomer and open dimer transition structures are summarized in Figure 1. Selected representations of optimized structures are depicted in Figure 11. Despite the potentially large perturbation caused by the chelate, we find surprisingly minor perturbations of the monomer and open dimer transition structure geometries relative to the simple *N*-alkylimines. We do note, however, a pronounced elongation of the chelating ligand−Li contacts relative to the monodentate solvent linkages in simple *N*-alkylimines.

Chelating Imine Metalations: Activation Enthalpies. Activation enthalpies for metalations of chelating imines **7**−**9** (Scheme 4) are detailed in Table 3. Both the monomer and open dimer transition structures are free of coordinated donor solvent and the predicted barriers for metalation share a common reactant structure. That is not say, however, that the monomer-open dimer preference is solvent-independent. The open dimer metalation requires two solvent dissociations per mole of product compared to a single dissociation per mole of product for the monomer metalation.

Metalations via chelated monomers show the characteristic acceleration due to increasing lithium amide bulk. Similarly, the solvent dependence for both acetone and pinacolone *N*-isopropylimine metalations show predicted rates that follow the order: NMe_3 > THF ≈ Me_2O > HMPA > H_2O. The more sterically demanding substrates exemplified by pinacolone-derived imine **9a** display substantially larger activation enthalpies than those containing the less hindered acetone imine **8**. The effect of the additional steric interaction imparted by the bulkier (branched) *N*-alkyl chelating appendage in **9b** increases the calculated activation enthalpies relative to the unbranched analog **9a**.

The chelated open dimer pathway is accelerated by increasing the steric bulk of the lithium amide base and displays the same solvent order as that described above for the chelated monomer pathway (NMe_3 > THF ≈ Me_2O > HMPA > H_2O). However, the requisite double solvent dissociation magnifies the differences in barrier heights. Consequently, the metalations involving double dissociation of NMe_3 are especially favorable while those requiring a double HMPA dissociation are unfavorable. The activation enthalpies are increased dramatically for the hindered pinacolone-derived substrates.

Comparisons of the monomer and open dimer metalation pathways (Table 3) reveal no simple trends. The open dimer pathway is preferred in the least hindered case (**7**, entry 1). The metalation of **8** with Me_2NLi/H_2O (entry 2) shows a contrasting preference for the monomer pathway. The monomer preference is more pronounced for LDA/H_2O than Me_2NLi/H_2O (cf. entries 2 and 4), while increasing the steric demands of the solvent (Me_2O vs. H_2O) causes the open dimer activation enthalpy to be smaller for LDA/Me_2O than Me_2NLi/Me_2O (entries 3 and 5). The influence of ligand lability is most clearly seen in the metalations by R_2NLi/NMe_3, in which the open dimer is dramatically preferred (entry 7). Consistent with this notion, metalations using R_2NLi/HMPA systems display a stronger monomer preference due to the high enthalpy of HMPA dissociation (entry 8). The increased bulk of the pinacolone imine **9a** acts to disproportionately retard the open dimer mechanism resulting in a relative promotion of the monomer mechanism (Table 3, entries 9−13). For the most severely hindered imine **9b** (Table 3, entries 14−18), only metalations by R_2NLi/NMe_3 retain a strong open dimer preference. The severe steric interaction caused by the added methyl substituent of **9b** appears to destabilize the open dimer transition structure more so than the monomer transition structure (cf. **27** and **28**); metalations of **9b** retain a modest open dimer preference only for the NMe_3 solvates.

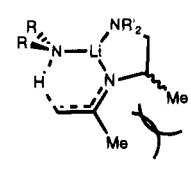

27

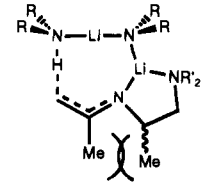

28

Discussion

Lithium dialkylamide-mediated metalations of ketones and imines were studied using semiempirical (MNDO) methods. The detailed survey of both monomer- and open dimer-based transition structure geometries and stabilities with variations in substrate, amide substituents, and coordinating solvent reveal a complex correlation of variables.

Transition Structure Geometries. We find minimal variation in the basic ring geometries of the monomer and open dimer metalation transition structures despite substantial changes in solvents and substituents. It is notable that the six-membered ring monomer transition structures (Figures 2 and 4) show little semblance to their carbocycle counterparts; the commonly cited "chairlike" six-centered transition structure[30a] finds no support. Similarly, the eight-membered ring open dimer transition structures (Figure 3 and 5) show little structural analogy with normal carbocycles.[44] It is widely accepted that a 90° H—C—C=O torsional angle corresponds to the optimum stereoelectronic alignment of the acidic C—H bond with the C=N or C=O p orbitals for proton abstraction.[42] This alignment is much more nearly attained in the open dimer transition structures than in the monomer transition structures. Thus, the open dimer transition structures appear to possess greater capacity to attain optimal deprotonation geometries.

Comparison of the imine with the ketone metalation transition structures reveals few differences in the basic geometries (Figure 1). However, *N*-alkyl moieties of the imines impose additional constraints. The *N*-alkyl moiety is buttressed by the substrate alkyl side chain on one side and the coordinated solvent on the other in both the monomer and dimer transition structures. The resulting steric effects appear to be the cause of dramatically lower kinetic acidities of imines relative to ketones (*vide infra*). We defer further discussion of the "*syn* effect" to a later section.

General Substituent and Solvent Effects on Reactivity. An understanding of relative aggregate reactivity requires an understanding of factors influencing both ground state and transition state energies. While this may seem obvious, discussions of organolithium reactivities often disproportionately focus upon the transition states, at times completely ignoring influences of variations in the ground state stabilities. Keeping in mind the truism that ground state *stabilization* can only serve to *decrease* the overall lithium amide reactivity, we note that previous computational studies of disolvated lithium dialkylamides show a dominance of steric effects.[8,9,51] For example, the stabilizing influence of the strongly dipolar, yet sterically demanding, HMPA ligand is markedly attenuated in the most severely hindered lithium amide dimers. The trialkylamine ligands (NMe_3) show marked sterically driven ground state destabilizations with consequent reductions in the activation barriers for both the monomer and open dimer pathways. The relief of the high steric strain is readily seen in comparisons of metalations mediated by Me_2NLi and LDA in which the increased bulk of the LDA causes lower metalation activation barriers (higher kinetic acidity).[1] The influence of solvent, dialkylamide, and substrate changes can now be evaluated by considering dependencies within the monomer and open dimer transition structures.

It appears that both monomer and open dimer transition structures afford substantial relief in the steric congestion that is characteristic of the lithium amide dimers. Thus, the maximum rates are observed for the most sterically demanding NMe_3 and HMPA ligands. In contrast to NMe_3, however, HMPA forms very strong metal—ligand interactions in uncongested environments. Thus, monomer-based ketone metalation rates are predicted to be high for NMe_3 solvates due to destabilizations (relative to ethereal ligands) that are more pronounced in the ground states than in the transition states. In contrast, the metalations involving HMPA ligands appear to benefit from limited ground state stabilization associated with high transition state stabilization. In the case of the open dimer-based mechanism, the energetic cost of dissociating an HMPA ligand coupled with the greater congestion at the transition structure (compared to the monomer structure) retards the metalations by the HMPA solvates relative to the NMe_3 solvates.

Relative Kinetic Acidities of Ketones and Imines. During the course of imine metalation rate studies, we were struck by the enormously reduced kinetic acidities of imines relative to ketones. Whereas cyclohexanone is metalated by LDA/THF within seconds at −90 °C, the half-life of the corresponding cyclohexanone *N*-isopropylimine is approximately 5 min at 0 °C. The MNDO calculations offer interesting insight into these widely differing reactivities. Metalations with unhindered H_2NLi/H_2O reveal little difference in the activation enthalpies for sterically undemanding imines and their isostructural ketone counterparts. However, as substituents are introduced into the substrate, base, and solvent to more appropriately model synthetically pertinent cases (e.g. LDA/**5**/THF), the calculated imine metalation barriers show a disproportionate increase commensurate with experiment. These differences appear to stem from the buttressing of the *N*-alkyl moiety by the *syn*-disposed imine side chain and the coordinated solvent (Figure 8a). The contrasting results from calculated enthalpies of minimally substituted and maximally substituted systems suggests two important conclusions: (1) the striking differences in reactivity between the ketones and *N*-alkylimines arise from the steric demands of the *N*-alkyl moiety rather than from electronic differences between C=O and C=N resonance stabilization, and (2) computational methods relying on gross structural simplifications—omission of substituents and solvents—are likely to be misleading.

Monomer vs Open Dimer Reactivity. The complex factors that influence the relative efficacies of the monomer and open dimer pathways are too numerous to reiterate. In general, however, we find that ketones are predicted to metalate via the open dimer pathway whereas imine metalations proceed more readily via monomers. LDA/**5a**/NMe_3 is the only base/*N*-alkylamine/solvent combination predicted to afford an overall preference for metalation via open dimers. Increased steric demands of the substrate promote the monomer pathway. This is logically ascribed to a decreased congestion in monomers relative to open dimers. However, this shift is inconsequential in ketone enolizations in that the open dimer pathway remains strongly preferred for the realistic solvents. The preference for monomer-based imine metalations is in strong agreement with *N*-alkylimine (and *N,N*-dimethylhydrazone) metalation rate studies;[3] the mechanism of lithium dialkylamide-mediated ketone metalation has not yet been determined.

Conventional wisdom suggests that organolithium aggregates undergo deaggregation to monomers prior to reacting with electrophiles.[16] However, there is mounting evidence that direct reactions of aggregates may occur more readily than originally suspected. For example, a number of imine and hydrazone metalation rate studies have implicated the monomer-based transition structures (**10**); however, the most *efficient* pathways (as defined by the relative pseudo-first-order rate constants) involve chelation-associated metalations via open dimer transition structures (**16**).[3c,d] A major portion of the results section

(51) For an early suggestion that steric effects are major determinants of solvation, see: Settle, F. A.; Haggerty, M.; Eastham, J. F. *J. Am. Chem. Soc.* **1964**, *86*, 2076.

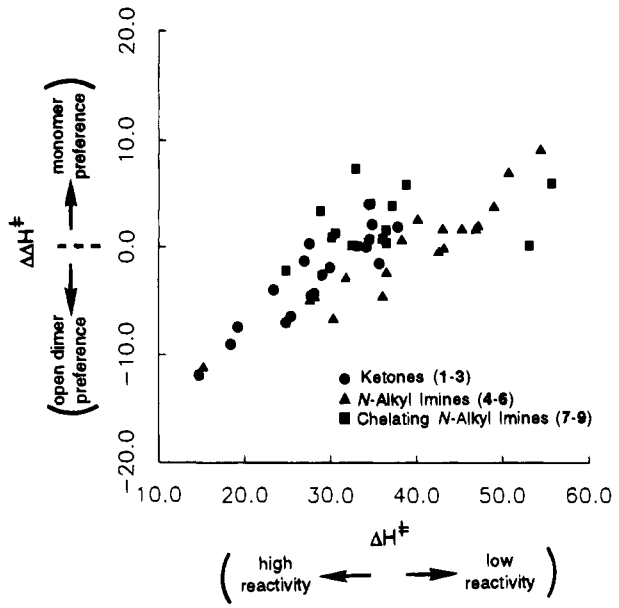

Figure 12. Relative open dimer-monomer preference ($\Delta\Delta H^{\ddagger}$) plotted as a function of the *lowest* predicted activation enthalpy ($\Delta H^{\ddagger}$). Data derive from all combinations of lithium amide/substrate/solvent combinations listed in Tables 1−3. $\Delta\Delta H^{\ddagger} = \Delta H^{\ddagger}_{(\text{open } d_{\text{imer}})} - \Delta H^{\ddagger}_{(\text{monomer})}$ (kcal/mol). The open dimer-based mechanism is preferred when $\Delta\Delta H^{\ddagger} < 0$.

delineates the many subtle structural features predicted to influence the relative reactivities of open dimers and monomers. As is often the case, complexity can obscure the simple principles. Figure 12 shows the relative propensities of the cyclic open dimer- and monomer-based mechanisms plotted as a function of the activation enthalpy of the lowest energy pathway available. The data derives from all ketone, *N*-alkylimine, and chelating imine substrates (Chart 1) for all solvent/substrate combinations (Tables 1−3). The trend is striking and the prediction is clear: *maximum reaction rates will be obtained by optimizing the open dimer rather than the monomer-based pathway.*

***E*/*Z* Enolization Selectivities.** Enolizations of 3-pentanone and related acyclic ketones have afforded benchmark selectivities for investigations of a wide range of lithium amide/solvent combinations.[30,31] One of the most notable observations is that THF-solvated lithium amides afford predominantly *E*-selective enolization while HMPA solvates afford *Z* selectivities. Although the chairlike transition structure (**24**) has served as a mnemonic to explain the *E* selectivities for almost 20 years, the MNDO studies indicate that the metalation transition structure bears little resemblance to a chair conformer. We became interested in determining whether MNDO could qualitatively reproduce the experimental results and whether the monomer−open dimer dichotomy might offer an explanation for the solvent dependencies. In general, we find a modest *E* selectivity for 3-pentanone enolization by cyclic monomer and open dimer mechanisms that is not only invariant with changes in solvent and lithium amide, but is also essentially the same for the two pathways.

This failure to detect *Z*-selective enolization could stem from a number of sources (independent of any shortcomings of MNDO) including enolate equilibration. However, several studies suggest that *Z* selectivities are kinetically derived.[6,49] We located acyclic transition structures corresponding to LDA monomer, open dimer, and triple ion fragments (**12**−**14**) with somewhat mixed results. On the one hand, it was gratifying to find a dominance of *Z* selectivities (as well as *syn* selectivities for imine metalations; *vide infra*). In addition, an unanticipated counterion desolvation in the triple ion without *concomitant substrate coordination* (Figure 7) offered a perspective of ion pairing and electrophilic catalysis[52] that we found to be very provocative. On the other hand, all acyclic transition structures proved to be quite destabilized relative to their cyclic counterparts. We do not known at this time whether this is a failure of the semiempirical method or the chemical models.

Overall, we feel that the calculations may offer a substantially improved physical model for the metalation leading to the *E* selectivities. It is unfortunate nonetheless that they do not offer an easily visualized mnemonic.

The "*Syn* Effect". The "*syn* effect" has been of some interest to us in light of investigations of the mechanism of imine and hydrazone metalations as well as lithioimine solution structures and reactivities. Despite the checkered history of the "*syn* effect" (*vide supra*), we can find no technical nor intellectual flaw in the experiments of Bergbreiter and Newcomb showing nearly isoenergetic *syn* and *anti* *N*-alkylimine metalations (eq 1).

The calculations suggest that *anti* metalations are marginally preferred relative to their *syn* counterparts for both cyclic monomer- and open-dimer-based metalations (Figures 8 and 9). Unfortunately, direct comparisons of *syn* and *anti* transition structure stabilities were clouded by anomalous (and difficult to assess) stabilization resulting from close C−Li and H−Li contacts unique to the monomer-based *syn* transition structures (Figure 8b). While this caused us to refrain from detailed investigations and discussions, we noted several features of the *syn* structures that are worthy of reiteration: (1) The *syn*-oriented monomer-based transition structures displayed a π interaction between the lithium and the two carbons of the $[C{=}CNR]^{\delta-}$ fragment (Figure 8b) akin to that proposed in the context of rate and mechanism studies; (2) the open dimer motif allows for *syn* metalations *without lithium−imine π complexation* that would be geometrically impossible with simple monomeric R_2NLi fragments (Figure 9b). This flexibility available to the R_2NLi open dimers was first noted by Schlosser in the context of LDA-mediated eliminations.[21] Limited investigations of *acyclic* transition structures via monomer, open dimer, and triple ion intermediates revealed *syn* preferences (e.g. Figure 10), yet all acyclic transition structures were substantially higher energy than their cyclic counterparts.

On the Role of Chelation. Unpublished computational studies of LDA revealed that chelating ligands such as TMEDA can impart a substantially greater stabilization to the monomer than the open dimer (eq 3). In contrast, rate studies revealed that imines such as **20** bearing potentially chelating pendant ligands can exhibit very high metalation rates due to inordinate acceleration of the *open dimer* pathway. Consistent with this notion, we find that the chelating imines are predicted to show a disproportionate acceleration of the open dimer-based metalation. This acceleration is attributable to a greater stabilization by chelation of the open dimer transition structure (eq 4). The calculations also confirm several other subtleties observed experimentally. For example, the chelation will be most influential for LDA bearing readily dissociated (minimally stabilizing) NR_3 ligands. We had also observed that inclusion of a methyl substituent on the imine *N*-alkyl moiety (**9a** vs **9b**)

(52) Jackman, L. M.; Dunne, T. S. *J. Am. Chem. Soc.* **1985**, *107*, 2805. Pierre, J.-L.; Handel, H. *Tetrahedron Lett.* **1974**, 2317. Loupy, A.; Seyden-Penne, J.; Tchoubar, B. *Tetrahedron Lett.* **1976**, 1677. Buncel, E.; Dunn, E. J.; Bannard, R. A. B.; Purdon, J. G. *J. Chem. Soc., Chem. Commun.* **1984**, 162. Chang. C. J.; Kiesel, R. F.; Hogen-Esch, T. L. *J. Am. Chem. Soc.* **1973**, *95*, 8446. Loupy, A.; Seyden-Penne, J. *Tetrahedron* **1980**, *36*, 1937.

markedly retards the open dimer pathway. This was readily traced to the buttressing within the substrate (**27** and **28**).

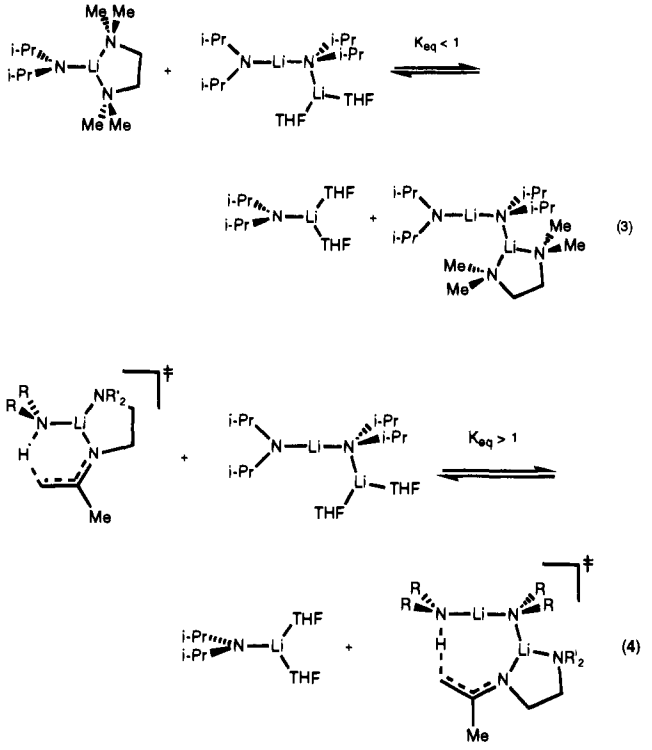

Conclusions

We have investigated metalations of ketones and imines using MNDO calculations. The studies were directed by NMR spectroscopic and rate studies implicating the precise transition structure stoichiometries. We also investigated pathways involving open dimer-like amide fragments. While open dimers are substantially less documented, recent computational,[8,9,22] spectroscopic,[6] crystallographic,[20] and kinetic studies[3] indicate that open dimers are both observable and kinetically important. The calculations allow us to explore the complex relationship of lithium amide, solvent, and substrate steric demands on the predicted absolute metalation rates as well as on the relative efficacies of the monomer- and open dimer-based pathways. The semiempirical computational method offered insights into a number of issues of general interest as summarized qualitatively in the discussion section. These include the *syn* effect observed in imine metalations, *E*/*Z* selectivities of ketone enolization, the dramatically reduced kinetic acidities of *N*-alkylimines relative to ketones, and the role of additional internal ligands on potentially chelating imine substrates.

The singularly dominant theme is that severe steric demands in the lithium dialkylamide-solvated dimer reactants is relieved by (1) the deaggregation en route to monomer transition structures or (2) the dimer ring opening and solvent dissociation en route to the open dimer-based transition structures. A number of important consequences that have not yet been explicitly discussed are worthy of elaborated as follows.

(1) Computational methods that rely on gross simplifications of the chemical model may necessarily exclude critical determinants of organolithium stabilities, reactivities, and selectivities. Detailed scrutiny using sophisticated Hartree Fock *ab initio* methods on overly simplistic models may not offer the most reliable comparison with experiment.[10]

(2) Many discussions of organolithium reactivity appear to ignore relative reactant stabilities as though they can be "normalized" (approximated as being equal). While modest reflection suggests that one simply cannot dismiss differences in ground state energies, the computations described herein go a step further by underscoring previous assertions[48] that structure and solvent-dependent variations in reaction rates often find their origins more in the ground states than in the transition states.

(3) Many discussions of relative reactivities and selectivities are couched in terms of transition structures with varying degrees of angle bending, bond stretching, and related "breathing" motions. Better solvents are often said to increase the "looseness" of transition structures, implying that a distribution of observable rates or selectivities are affiliated with a continuum of geometry changes. Granted, the optimized reactant and transition structure geometries show detectable substituent- and solvent-dependencies; however, we find it more productive to think of substituents and solvents as modulating the relative *stabilities rather than the geometries* of the transition structures for two or more competing reaction pathways.

(4) Monomers are often cited as the most reactive organolithium aggregation states. It is difficult to assess the relative "reactivities" of monomers and aggregates without becoming entangled in semantics that stems for translation of the mathematics of thermochemistry to prose. However, we can state without much difficulty that the calculations described above and previous rate studies[3] suggest that the *maximum* rates may be attainable by optimizing the open dimer-based pathway. This highlights a potential distortion in the organolithium mechanistic picture stemming from organolithium rate studies. It is possible that the judicious choice of substrate, solvent, and temperature required to slow the rates for convenient monitoring inadvertently precludes detection of the most efficient—*the most important*—reaction pathways.

Acknowledgment. We thank the National Institutes of Health for direct support of this work. The computational studies were conducted using the Cornell National Supercomputer Facility, a resource of the Center for Theory and Simulations in Science and Engineering (Cornell Theory Center), which receives major funding from the National Science Foundation and IBM Corporation, with additional support from New York State and members of the Corporate Research Institute.

JA942303X